Chapter 5

Growth plate regulation and osteochondroma formation: insights from tracing proteoglycans in zebrafish models and human cartilage

Carlos E de Andrea, Frans A Prins,
Malgorzata I Wiweger and Pancras CW Hogendoorn
Journal of Pathology 2011; 224:160-168

Abstract

Proteoglycans are secreted into the extracellular matrix of virtually all cell types and function in several cellular processes. They consist of a core protein onto which glycosaminoglycans (e.g., heparan or chondroitin sulphates), are attached. Proteoglycans are important modulators of gradient formation and signal transduction. Impaired biosynthesis of heparan sulphate glycosaminoglycans causes osteochondroma, the most common bone tumour to occur during adolescence. Cytochemical staining with positively charged dyes (e.g., polyethyleneimine—PEI) allows, visualisation of proteoglycans and provides a detailed description of how proteoglycans are distributed throughout the cartilage matrix. PEI staining was studied by electron and reflection contrast microscopy in human growth plates, osteochondromas and five different proteoglycan-deficient zebrafish mutants displaying one of the following skeletal phenotypes: *dackel* (*dak/ext2*), lacking heparan sulphate and identified as a model for human multiple osteochondromas; *hi307* (β*3gat3*), deficient for most glycosaminoglycans; *pinscher* (*pic/slc35b2*), presenting with defective sulphation of glycosaminoglycans; *hi954* (*uxs1*), lacking most glycosaminoglycans; and *knypek* (*kny/gpc4*), missing the protein core of the glypican-4 proteoglycan. The panel of genetically well-characterized proteoglycan-deficient zebrafish mutants serves as a convincing and comprehensive study model to investigate proteoglycan distribution and the relation of this distribution to the model mutation status. They also provide insight into the distributions and gradients that can be expected in the human homologue. Human growth plate, wild-type zebrafish and fish mutants with mild proteoglycan defects (*hi307* and *kny*) displayed proteoglycans distributed in a gradient throughout the matrix. Although the mutants *pic* and *hi954*, which had severely impaired proteoglycan biosynthesis, showed no PEI staining, *dak* mutants demonstrated reduced PEI staining and no gradient formation. Most chondrocytes from human osteochondromas showed normal PEI staining. However, approximately 10% of tumour chondrocytes were similar to those found in the *dak* mutant (e.g., lack of PEI gradients). The cells in the reduced PEI-stained areas are likely associated with loss-of-function mutations in the *EXT* genes, and they might contribute to tumour initiation by disrupting the gradients.

Keywords: growth plate; osteochondroma; proteoglycans; heparan sulphate; gradients; exostosis; zebrafish; bone tumours

Introduction

Bone formation and development are governed by gradients of signalling molecules, which trigger specific cell responses. Proteoglycans are important modulators of gradient formation and signal transduction [1,2]. They are found in the extracellular matrix and attached to the cell membrane in virtually all types of tissue [2]. Proteoglycans are composed of highly diverse core proteins to which one or more glycosaminoglycans chains are covalently linked at specific sites (Figure 1). Glycosaminoglycans are unbranched polysaccharides that consist of a backbone of repeating disaccharide units, often containing negatively charged sulphate groups [3]. Some proteoglycans have only one glycosaminoglycan chain (e.g., decorin), whereas others have more than one hundred chains (e.g., aggrecan). For example, heparan sulphate proteoglycans are composed of diverse core proteins onto which two or three heparan sulphate glycosaminoglycan chains are attached.

Bone lengthening occurs in the epiphyseal growth plate, a specialised cartilage structure found at the ends of long bones. Bone elongation is achieved through successive rounds of growth plate chondrocyte divisions, matrix secretion, hypertrophy, apoptosis, calcification and replacement with mineralised. Growth plate regulation requires signalling molecules, such as members of the Wingless (Wnt/Wg), Hedgehog (Hh), Transforming growth factor-β (TGFβ), Bone morphogenetic protein (BMP) and fibroblast growth factor (FGF) families [4]. Many of these molecules bind proteoglycans, heparan sulphate proteoglycans in particular. Proteoglycans influence the distribution of these signalling molecules in the extracellular matrix, their receptor-binding affinity and the responses of cells to secreted protein factors [2]. Although studies have shown that several signal transduction pathways rely on gradients established by the proteoglycan distribution [5,6], it is still unclear how these gradients are formed and shaped.

Mutations affecting the biosynthesis of either proteoglycan or glycosaminoglycan are the cause of several human disorders. Loss-of-function mutations in the *EXT1* (8q24.1) and *EXT2* (11p11) tumour suppressor genes have been linked to osteochondromas [7–10]. *EXT1* and *EXT2* encode type II transmembrane glycosyltransferases 11, which localise to the endoplasmic reticulum and Golgi complex. EXT1 and EXT2 form an oligomeric complex that catalyses the elongation of heparan sulphate glycosaminoglycan chains [3, 12]. Therefore, the impairment of heparan sulphate glycosaminoglycan chain elongation is thought to be the initiating event for osteochondroma formation.

Osteochondromas are the most common benign bone tumours of adolescence [13]. They are characterised by sporadic (non-familial/solitary) or multiple (hereditary) cartilage-capped bony projections from the metaphyses of endochondral bones adjacent to the growth plate and develop during skeletal growth [14]. Multiple osteochondromas, previously called hereditary multiple exostoses, result from an autosomal dominant disorder, with a prevalence of 1 in 18 000 [15]. Patients with multiple osteochondromas are short in

stature and have bowed bones that can restrict movement and ultimately result in joint dislocation [15]. In contrast, patients with sporadic lesions may develop symptoms on the affected side. Sporadic and multiple lesions are morphologically indistinguishable [14].

Model systems have provided significant insight into osteochondroma pathogenesis and show a detailed picture of the role of heparan sulphate proteoglycans in tumour formation. Reduced EXT1 and EXT2 co-polymerase activity results in the production of short heparan sulphate chains [16]. Short chains decrease fibroblast growth factor 2 signal transduction, which may impair chondrocyte differentiation. The zebrafish *dackel* (*dak/ext2*) mutant has a cartilage phenotype that strongly resembles that of human osteochondromas. *dak* cells transplanted into wild-type zebrafish cartilage behave normally when juxtaposed with wild-type cells and abnormally when implanted at the edge of cartilage [17]; these results indicate that *ext*-null cells are not autonomous and that the secretion of heparan sulphate proteoglycans from the neighbouring wild-type cells is able to rescue the mutant cells within the chondrocyte stack. However, at the edge of the cartilage elements, where the level of heparan sulphate proteoglycans is decreased, *ext*-null chondrocytes start to form outgrowths [17]. These outgrowths suggest that a pool of mutant chondrocytes at a specific location in the growth plate is required to escape the proteoglycan gradient generated by neighbouring cells and give rise to osteochondromas. Recent studies using Cre recombinase drivers to generate *Ext1* knockouts in mouse skeletal cells show that somatic loss of the wild-type *Ext1* allele is needed for osteochondroma formation. Loss of heterozygosity has also been detected in a subset of human sporadic and multiple osteochondromas [8,10,18, 19]. Interestingly, during tumour formation in mice, wild-type chondrocytes are recruited from the growth plate or the neighbouring tissue to generate a non-clonal population of cells [20,21]. Given that cells require a certain threshold level and distribution of heparan sulphate proteoglycans to grow properly, the wild-type chondrocytes may create an environment conducive for *EXT1*$^{-/-}$ cells to proliferate and form a tumour [22]. We previously reported that growth plate-like polarity was retained in subpopulations of osteochondroma cells, which may also indicate the presence of a heterogeneous cell composition in human osteochondromas [23].

Despite all of the progress in the understanding of the pathogenesis of osteochondroma, many questions remain unanswered: (a) how do the null-*EXT1* cells give rise to an osteochondroma; and (b) what is the proteoglycan distribution in osteochondromas that are present within the cartilaginous matrix? Proteoglycans can be localised with an electron microscope using positively charged, electron-dense dyes. Polyethyleneimine (PEI) is a well-described cationic dye that binds to anionic sites, allowing visualisation and quantification of negatively charged sites of proteoglycans in cartilage and other tissues at the ultrastructural level [24–27]. Using electron and reflection contrast microscopy, we analysed the overall distribution of proteoglycan anionic sites in human growth plates,

osteochondromas and five different proteoglycan-deficient zebrafish mutants displaying a skeletal phenotype. The panel of genetically well-characterised proteoglycan-deficient zebrafish mutants served as a convincing and comprehensive study model to investigate proteoglycan distribution and provided insights into the distribution and gradients that could be expected in the human homologue. Our results provide clues to understand the biology of the growth plate and the pathogenic mechanism of osteochondroma by demonstrating the presence of the proteoglycan gradient through the cartilage matrix and its focal loss in tumours.

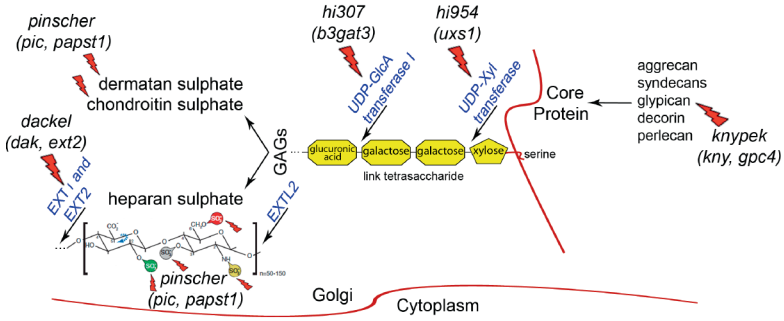

Figure 1. Schematic representation of proteoglycan biosynthesis, showing the specific steps in which the five homozygous zebrafish mutants (italics) are affected.

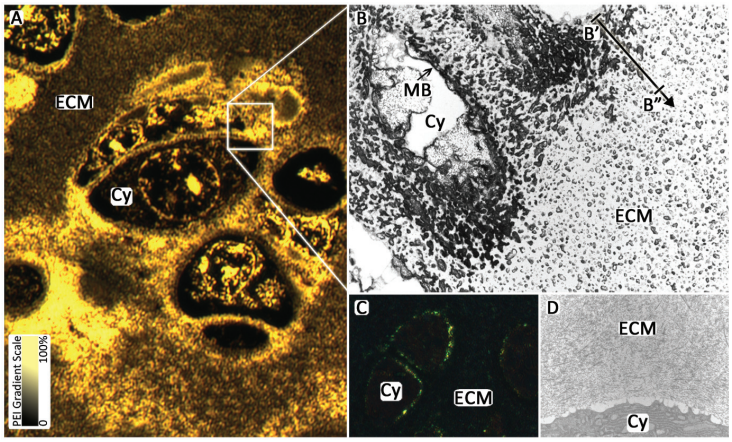

Figure 2. Spatial distribution of polyethyleneimine (PEI) in the normal human growth plate. The distribution of anionic sites by PEI was evaluated by reflection contrast (A) and electron microscopy (B). A concentration gradient of electron-dense deposits of PEI (black) is observed as a function of distance through the cartilage (B′ to B″). Negative controls show no PEI-positive structures in either the electron micrographs (C) or the reflection contrast image (D). CY, cytoplasm; MB, cell membrane; ECM, extracellular matrix. Magnifications: (A) × 110; (B) × 10 000; (C) × 100; (D) × 20 000.

Materials and methods

Animals

Zebrafish (*Danio rerio H.*) embryos were obtained by natural crosses and staged in accordance with Kimmel et al. [28]. Wild-type and five null mutants were selected: *dackel* (*dak*), *exostoses (multiple) 2*; *pinscher* (*pic/slc35b2*), *solute carrier family 35, member B2* (previously named *PAPS transporter 1*, *papst1*); *hi307*, β-*1,3-glucuronyltransferase 3*; *hi954*, *UDP-glucuronic acid decarboxylase 1*; and *knypek* (*kny*) *glypican 4*. Zebrafish were raised until 5-days post-fertilization. Each homozygous mutant line has been previously characterised [29]. Prior to these experiments, the fish were anaesthetised in Tricane, and the homozygous mutants were sorted by phenotype.

Human cartilage

Two postnatal growth plates and two osteochondromas were obtained from surgical specimens at the Leiden University Medical Centre. One osteochondroma (L-2999) was a sporadic lesion from a 16 year-old patient. The other (L-2675) was a lesion from a 32 year-old patient with multiple osteochondromas, confirmed in multidisciplinary discussions of the case by the National Bone Tumour Committee according to the Dutch guidelines. The growth plates were from orthopaedic resections for pathological conditions not related to osteochondroma. All samples were handled in a coded fashion, and all procedures were performed according to the ethical guidelines of the Code for Proper Secondary Use of Human Tissue in The Netherlands (Dutch Federation of Medical Scientific Societies).

Tissue preparation

The method of tissue preparation has been described previously [24–26,30]. Anionic sites in zebrafish cartilage, human growth plate and osteochondroma were labelled by tissue incubation in polyethyleneimine (PEI; PEI-600, Polysciences, Warrington, PA, USA), a synthetic polymer that is highly cationic and water-soluble and forms an electron-dense insoluble product upon reaction with osmic acid. Two methods were applied: (a) the PEI pre-embedding method, where PEI incubation precedes tissue fixation; and (b) the PEI post-embedding method, where PEI incubation follows fixation in 2.5% glutaraldehyde in 0.1 m sodium cacodylate buffer, pH 7.4, for 1 h. Freshly collected tissues were incubated with 1% PEI in sodium cacodylate buffer at a pH of 7.4 or 1.0, each for 6 or 12 h, with constant agitation. After incubation, the samples were washed three times in sodium cacodylate buffer and fixed and/or stained with 2% phosphotungstic acid and 1% glutaraldehyde for 1 h. Next, they were washed three times in sodium cacodylate buffer, fixed in 1% osmic acid and embedded in Epon. For the negative controls, the samples were incubated in sodium cacodylate buffer without PEI.

Morphological techniques

Ultrathin sections of zebrafish cartilage, human growth plate and osteochondroma were obtained for each experimental condition and briefly stained with phosphotungstic acid. Two fish were analysed from each line. Sequential sections were placed on glass slides for reflection contrast microscopy or on grids for electron microscopy. The preparations were examined under a Leitz Orthoplan microscope (Leitz, Wetzlar, Germany) equipped for epi-illumination, which was adapted for reflection contrast microscopy as described previously [31]. The slides were examined under a 100× objective lens. A JEOL JEM-1011 electron microscope equipped with a MegaView III digital camera was used for ultrastructural analysis.

Data analysis

For gradient analysis, the electron-dense deposits of PEI were plotted using ImageJ software, version 1.41h (National Institutes of Health, Bethesda, MD, USA). The plot profile represents the intensity of pixels along a line within a selected area in the cartilage, starting from the cell surface and moving to the periphery/neighbouring cell. The x axis shows the distance through the selection and the y axis the average pixel intensity, in which 0 is black and 255 is white.

Results

Distribution of the proteoglycan anionic sites in cartilage

PEI deposition was evaluated by electron and reflection contrast microscopy in zebrafish and human cartilage (Figure 2). Wild-type zebrafish and proteoglycan-deficient mutants were used to determine the optimal conditions for studying the distribution of anionic sites in cartilage and the specificity of binding at the given condition. PEI post-embedding methods showed a virtual absence of stained anionic sites at different pH levels (see Supporting information, Figure S1). In contrast, PEI pre-embedding methods revealed that the decrease in the number of stained anionic sites followed the reduction in the pH level, thereby reflecting the charge-dependent specificity of its binding. The PEI pre-embedding method usually affects the preservation of cell components. However, at pH 7.4, PEI staining provided good cell preservation and excellent contrast within the cartilage matrix. As a result, this condition was used for further studies. Electron-dense deposits were observed throughout the extracellular matrix, and they outlined branched, round to oval, winding structures (Figures 2,3). To confirm the binding of PEI to the anionic sites of the proteoglycans, zebrafish mutants with impaired proteoglycan synthesis were used. PEI-positive structures were found in the extracellular matrix in wild-type fish and in the cartilage of mutant fish that lacked the glypican 4-core protein (*kny/gpc4*) or some glycosaminoglycans (*hi307/b3gat3*). No PEI staining was observed, either in mutants that were unable to add negatively charged sulphate groups to glycosaminoglycans (*pic/slc35b2*) or in ones that lack most of the glycosaminoglycans (*hi954/uxs1*) (Figure 3). The same results were obtained 6 and 12 h

after incubation with PEI. Nuclear staining was present in all fish lines analysed and was most likely due to negatively charged phosphate ions present in the DNA structure [32].

Gradients of proteoglycans in cartilage

PEI-positive aggregates were identified in the cytoplasm and in the extracellular matrix of wild-type zebrafish cartilage. Large and densely packed cytoplasmic aggregates of proteoglycans were found in close contact with the plasma membrane (Figure 3). In the matrix of the wild-type, *kny* (*gpc4*) and *hi307* (β*3gat3*) zebrafish mutants, there was a broader variation in the diameter of the PEI aggregates (Figure 3). Additionally, the aggregates resembled vesicles, which enclosed electron-dense deposits of PEI and were filled in with less densely packed deposits (Figure 3, arrowheads). The plot profile of the electron micrographs shows the gradient formation (Figure 4), in which the diameter of the PEI aggregates decreased with the distance from the cell surface. Although the human growth plate has a more complex organisation compared with fish cartilage, similar PEI distribution patterns were identified (Figure 5). Contrast-reflection images showed that all analysed cells in the growth plate (n = 64) were surrounded by PEI-positive aggregates (Figure 5). Growth plate chondrocytes are classically divided into three distinct zones: resting, proliferating and hypertrophic [23]. No differences between those zones were observed. The plot profiles of the electron micrographs showed gradient formation between columns of chondrocytes in the growth plate (Figure 5, cell–matrix plot profile). However, no gradient was found between cells within a column (Figure 5, cell–cell plot profile).

Reduction in proteoglycan aggregates and no gradient formation in Ext mutant chondrocytes

The homozygous *dak* zebrafish mutant, which has a mutation in the homologue of the human *EXT2* gene, has a cartilage phenotype that resembles that of osteochondroma [17]. Reduced PEI staining was observed in this mutant. Small electron-dense deposits of PEI were found homogeneously distributed throughout the extracellular matrix (Figure 4). Reflection contrast images demonstrated a reduction in PEI staining in all cells of the cartilage elements (n = 84). PEI deposits were often observed in the nucleus of these cells and in the endoplasmic reticulum (Figure 3). The plot profile of the electron micrographs showed a prominent reduction in PEI aggregates and no gradient formation (Figure 4).

Scattered proteoglycan distribution in osteochondroma

In both sporadic and multiple osteochondromas, contrast reflection microscopy showed that the majority of cells were surrounded by PEI-positive matrix (n = 53/59) (Figure 6A,C). The plot profile of the electron micrographs demonstrated gradient formation similar to that observed in wild-type zebrafish and in the human growth plate (Figure 5).

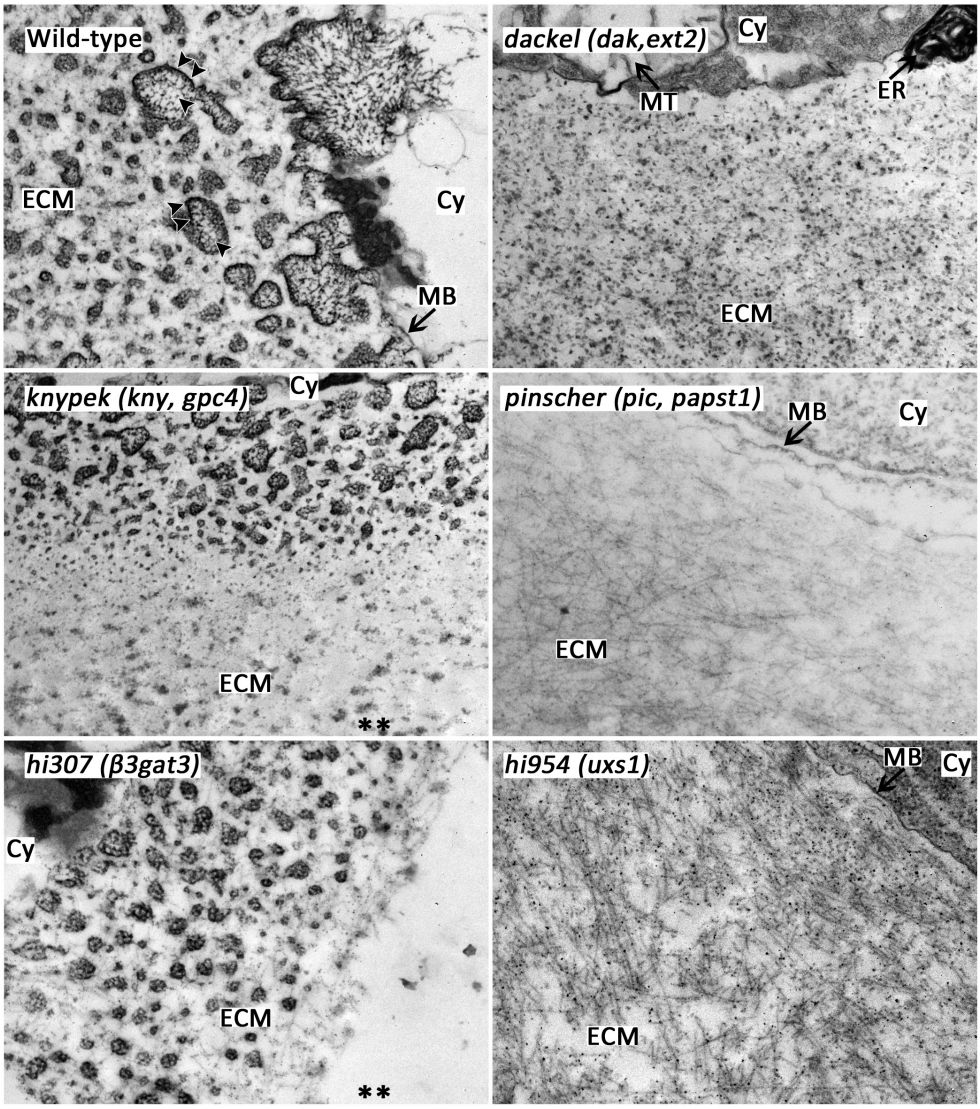

Figure 3. The distribution of proteoglycans in the zebrafish cartilage in wild-type and proteoglycan-deficient homozygous mutants. Electron-dense deposits of PEI were found in the cytoplasm (Cy) and accumulated in the endoplasmic reticulum (ER) and the extracellular matrix (ECM). In the wild-type zebrafish, *kny* and *hi307* PEI staining revealed a gradient. No PEI staining was observed in the mutants with severe impairment of proteoglycan biosynthesis, *pinscher* (*pic*) and *hi954*. Reduced PEI staining was identified in heparan sulphate–deficient *dackel* (*dak*) mutants. PEI aggregates often formed vesicle-like structures, enclosed in a line of electron-dense deposits (wild-type, two arrowheads) containing, in its interior, more loosely packed deposits (wild-type, arrowhead). MB, cell membrane; MT, mitochondria; **, edge of the cartilage. All electron micrographs are × 40 000.

However, approximately 10% of osteochondroma cells (n = 6/53) resembled dak chondrocytes (Figure 6A,B,D,E). Both contrast-reflection and electron micrographs showed a scattered distribution of proteoglycans and a prominent reduction in PEI aggregates in the matrix surrounding these cells (Figure 5). The plot profile indicated that no gradients were formed around small populations of osteochondroma cells. This finding suggests the presence of both normal and proteoglycan-deficient cells in the cartilage cap (Figure 6A,C).

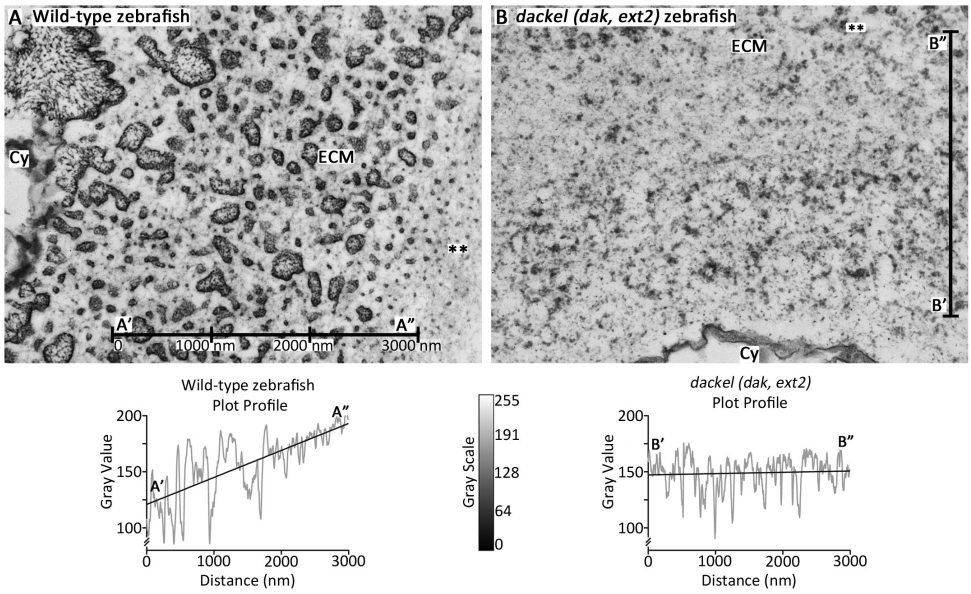

Figure 4. The distribution of proteoglycans shows gradients in the normal cartilage and a lack of gradient in *dackel* (*dak/ext2*) zebrafish mutants. The line of the plot profile in wild-type zebrafish demonstrates a decrease in PEI staining intensity from A' to A", which reflects gradient formation. The plot profile in the *dackel* (*dak/ext2*) mutant shows a prominent reduction of PEI staining intensity and an absence of gradient (from B' to B"). The PEI staining in dackel is similar to that found in the region close to the edge of the cartilage (**) of wild-type zebrafish. Cy, cytoplasm; ECM, extracellular matrix. All electron micrographs are × 30 000.

Discussion

We demonstrated a cytochemical method for the visualisation and quantification of negatively charged proteoglycan-associated sites in cartilage and confirmed this finding by observing an absence of PEI staining in zebrafish variants with severely impaired proteoglycan biosynthesis: *pic* (*slc35b2*) and *hi954* (*uxs1*). At pH 7.4, the PEI staining pattern in the cartilage matrix of the growth plate and of wild-type zebrafish was similar to that observed in epiphyseal and osteoarthritic cartilage, which has been previously reported [26,33].

Regular histochemical stains (e.g., alcian blue) notoriously demonstrate different compositions, organisation of proteoglycans [34,35] and the presence of pericellular, territorial and interterritorial matrix compartments in cartilage [36]. The pattern of PEI staining also reflects a diverse proteoglycan distribution. The overall distribution of proteoglycans in gradients, as shown by PEI staining, may be either the cause or the consequence of the formation of compartments in cartilage. In any case, proteoglycans are well known to play a role in the physiological regulation and homeostasis of cartilage.

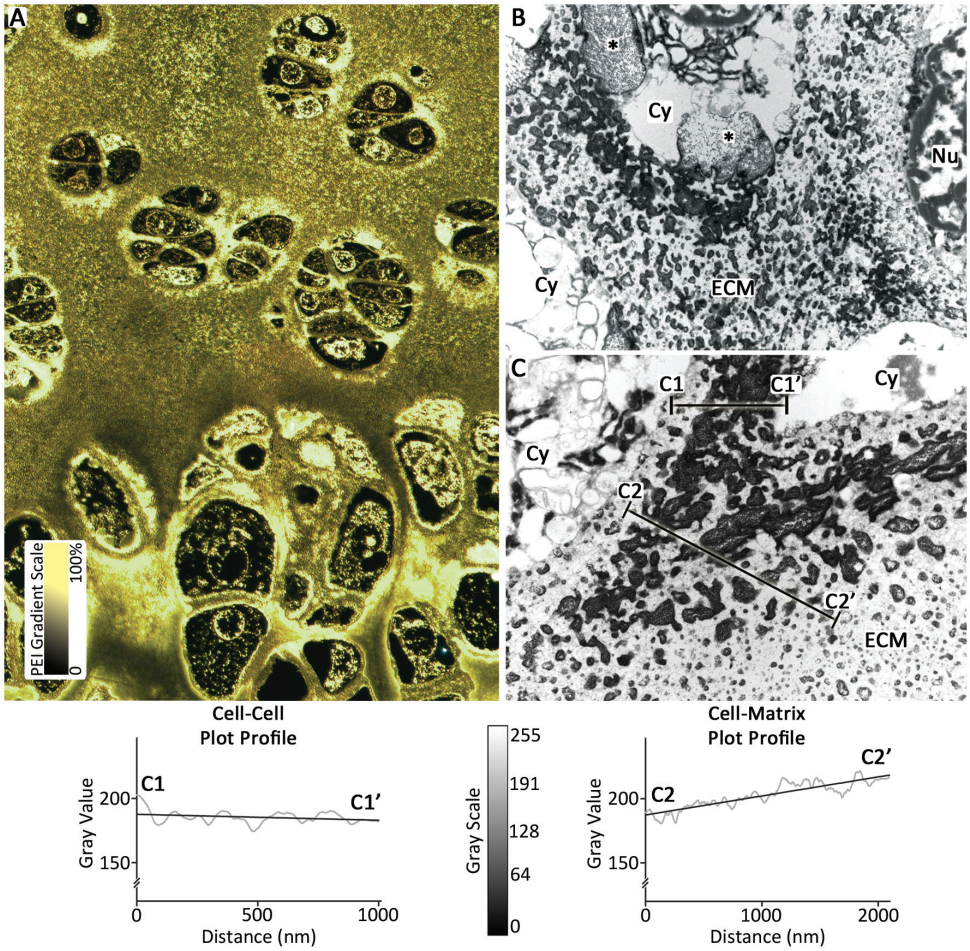

Figure 5. The distribution of proteoglycans in the growth plate. Contrast-reflection images (four pictures shown together) (A) show all cells surrounded by PEI staining. Electron-dense deposits of PEI are found in the cytoplasm (Cy) (B, *) and in the extracellular matrix (ECM) (A–C). The plot profile of the electron micrographs demonstrates a larger gradient formation from C2 to C2′ in the peripheral region (between columns of cells, cell–matrix plot profile) and a smoother gradient from C1 to C1′ in the region inside the column (between cells of the same column, cell–cell plot profile). Nu, nucleus. Magnifications: (A) × 90; (B) × 10 000; (C) × 20 000.

The distribution of proteoglycans in zebrafish cartilage is neither affected by a lack of glypican-4 (*kny* mutant), nor a GPI-anchored cell surface heparan sulphate proteoglycan, nor by the absence of UDP–Gal transferase I (*hi307* mutant). This enzyme, encoded by β*3gat3*, is involved in the construction of the tetrasaccharide linkage region required for heparan, chondroitin and dermatan sulphate biosynthesis (Figure 1).

The development of the growth plate and its regulation are controlled by morphogen gradients (reviewed in 3). Heparan sulphate proteoglycans one of the essential regulators for morphogen gradient formation [6]. In this study, the gradient formed by proteoglycans is hypothesised to be involved in such regulation. The vesicle-like aggregates visualised by PEI staining might be related to a gradient formation of signalling molecules. The concentration of a given proteoglycan-binding molecule might be associated with the size of the aggregates at a certain position across the matrix. For example, the dilution of a signalling molecule increases with the distance from the cell surface, following the decrease in size of the proteoglycan aggregates. Proteoglycans in secretory vesicles have been described as having a role in packaging granular contents, maintaining enzymes (e.g., proteases) in an active state and regulating various tissue homeostasis-related biological activities after secretion [37].

Recent studies have shown that the cartilage cap of mouse osteochondromas is a mosaic of wild-type chondrocytes and cells lacking functional *Ext1* [20,21]. Here we demonstrate, using PEI staining, that human osteochondromas have a heterogeneous composition of both normal and proteoglycan-deficient cells. Approximately 10% of osteochondroma cells showed a prominent reduction in PEI aggregates in the surrounding matrix, with no gradient formation. Similar patterns were observed in the cartilage of *dackel*, the zebrafish homologue of human multiple osteochondromas. The human osteochondroma cells in the reduced PEI staining areas are likely associated with loss-of-function mutations in the *EXT* genes. Taken together, these findings provide major insight into human osteochondromagenesis. Cells in the growth plate or in the neighbouring tissue harbouring homozygous mutations in *EXT1/2* disrupt the diffusion gradients and signal transduction, which may contribute to tumour initiation. Reflection contrast images of osteochondromas show a reduction, but not an absence, of proteoglycans in the pericellular region of the proteoglycan-deficient cells. It is well described that the *EXT1*-null mutation in mice is embryonic lethal [22], and *EXT1*-null cells are difficult to grow in culture [18]. Therefore, a certain threshold level of heparan sulphate seems to be critical for *EXT1*-null cell survival. The integration of wild-type chondrocytes into the osteochondroma cap could provide an environment conducive to tumour cell proliferation and development. The ability of mutant cells to recruit normal cells to participate in the formation of a lesion is well described in fibrous dysplasia of the bone [38].

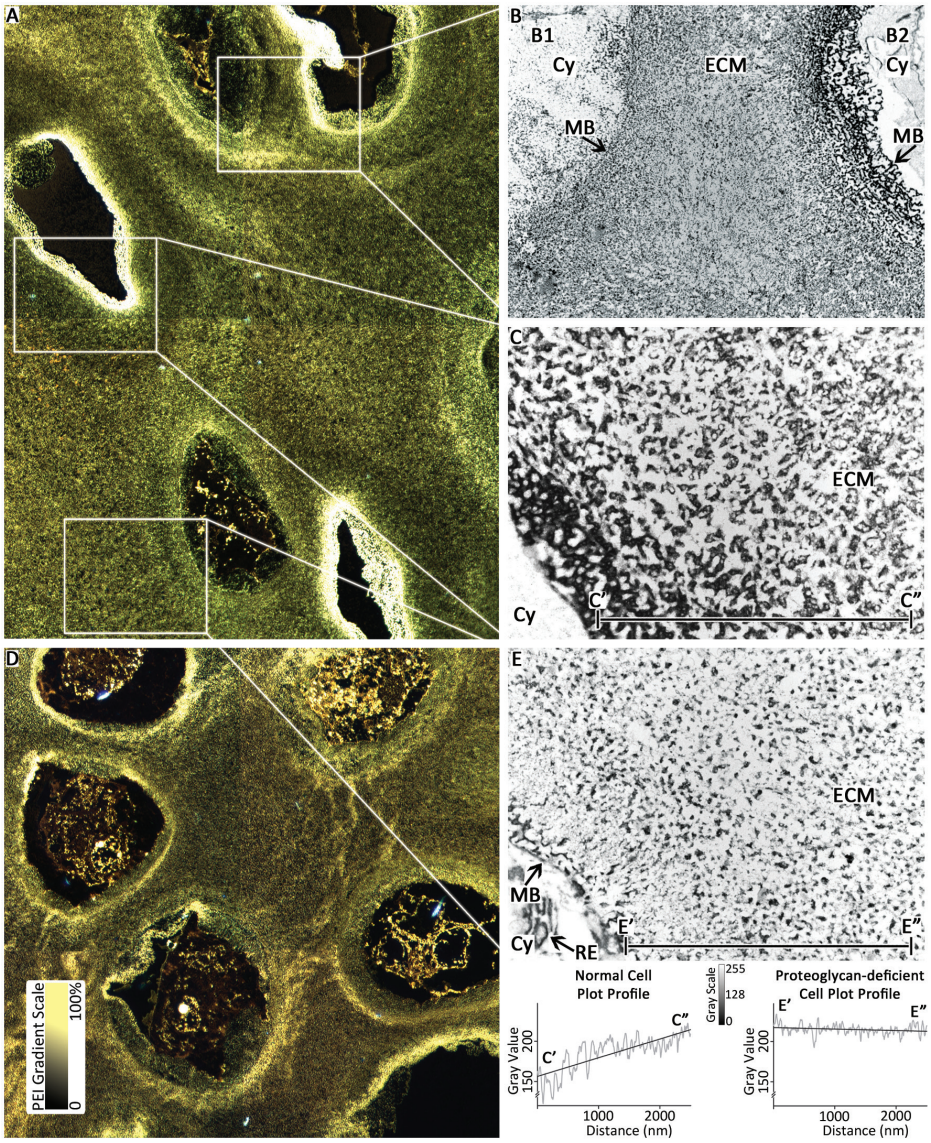

Figure 6. The scattered distribution of proteoglycans in osteochondroma. Contrast reflection images (CRI, four pictures shown together) (A, D) show cells surrounded by PEI staining and unstained cells. Electron micrographs (B, C, E) taken from similar areas of the CRI represent two neighbouring cells (B), in which one cell (B2) has a normal distribution of PEI and the other (B1) has a reduction in PEI staining. The normal cells (C) show gradient formation of electron-dense deposits of PEI from C′ to C″ as a function of distance through the cartilage (normal cell plot profile). Proteoglycan-deficient cells (E) demonstrate few PEI aggregates and no gradient formation from E to E″ (proteoglycan-deficient cell plot profile); electron-dense deposits of PEI were observed in the endoplasmic reticulum (RE) (E). Cy, cytoplasm; MB, cell membrane; ECM, extracellular matrix. Magnifications: (A, D) × 90; (B) × 6000; (C, E) × 20 000.

Although these data significantly advance our understanding of growth plate regulation and the pathogenesis of osteochondroma, a number of questions remain. For instance, how are macromolecules trafficked across the extracellular matrix of the growth plate? How does the mixture of both normal and proteoglycan-deficient cells explain the severity of the phenotype in patients with multiple osteochondromas? Is this mixture of cells homogenously present throughout the tumour? How are proteoglycans distributed in osteochondroma cases that have functional *EXT1/2*? In any event, this study clearly demonstrates the existence of proteoglycan gradients within the growth plate and an absence of this gradient around a subset of osteochondroma cells, which affects the diffusion of signalling molecules and implies a distinct role in the pathogenic mechanisms of tumour formation.

Acknowledgements

This work was supported by the European Network of Excellence EuroBoNeT (http://www.eurobonet.eu), Grant No. 018814 (LSHC-CT-2006-018814).

Author contributions

CEdeA and PCWH were involved in the study design; CEdeA, MIW and FAP collected the data; CEdeA, MIW and PCWH analysed and interpreted the data; MIW, CEdeA and PCWH carried out literature searches; CEdeA and FAP generated the figures. All authors were involved in writing the paper and had final approval of the submitted and published versions.

References

1. Yan D, Lin X. Shaping morphogen gradients by proteoglycans. Cold Spring Harbor Perspect Biol 2009; 1: a002493.
2. Hacker U, Nybakken K, Perrimon N. Heparan sulphate proteoglycans: the sweet side of development. Nat Rev Mol Cell Biol 2005; 6: 530–541.
3. Bulow HE, Hobert O. The molecular diversity of glycosaminoglycans shapes animal development. Annu Rev Cell Dev Biol 2006; 22: 375–407.
4. Kronenberg HM. Developmental regulation of the growth plate. Nature 2003; 423: 332–336.
5. Wu Y, Belenkaya TY, Lin X. Dual roles of Drosophila glypican Dally-like in Wingless/Wnt signaling and distribution. Methods Enzymol 2010; 480: 33–50.
6. Cortes M, Baria AT, Schwartz NB. Sulfation of chondroitin sulfate proteoglycans is necessary for proper Indian hedgehog signaling in the developing growth plate. Development 2009; 136: 1697–1706.
7. Bovee JVMG, Hogendoorn PCW, Wunder JS, et al. Cartilage tumours and bone development: molecular pathology and possible therapeutic targets. Nat Rev Cancer 2010; 10: 481–488.

8. Hameetman L, Szuhai K, Yavas A, et al. The role of EXT1 in non hereditary osteochondroma: identification of homozygous deletions. J Natl Cancer Inst 2007; 99: 396–406.
9. Wuyts W, Van Hul W. Molecular basis of multiple exostoses: mutations in the EXT1 and EXT2 genes. Hum Mutat 2000; 15: 220–227.
10. Bovee JVMG, Cleton-Jansen AM, Wuyts W, et al. EXT-mutation analysis and loss of heterozygosity in sporadic and hereditary osteochondromas and secondary chondrosarcomas. Am J Hum Genet 1999; 65: 689–698.
11. McCormick C, Leduc Y, Martindale D, et al. The putative tumour suppressor EXT1 alters the expression of cell-surface heparan sulfate. Nat Genet 1998; 19: 158–161.
12. Zak BM, Crawford BE, Esko JD. Hereditary multiple exostoses and heparan sulfate polymerization. Biochim Biophys Acta 2002; 1573: 346–355.
13. van den Berg H, Kroon HM, Slaar A, et al. Incidence of biopsy-proven bone tumors in children: a report based on the Dutch pathology registration 'PALGA'. J Pediatr Orthop 2008; 28: 29–35.
14. Khurana J, Abdul-Karim F, Bovée JVMG. Osteochondroma. In World Health Organization Classification of Tumours. Pathology and Genetics of Tumours of Soft Tissue and Bone, Fletcher CDM, Unni KK, Mertens F (eds). IARC Press: Lyon, France, 2002; 234–236.
15. Stieber JR, Dormans JP. Manifestations of hereditary multiple exostoses. J Am Acad Orthop Surg 2005; 13: 110–120.
16. Osterholm C, Barczyk MM, Busse M, et al. Mutation in the heparan sulfate biosynthesis enzyme EXT1 influences growth factor signaling and fibroblast interactions with the extracellular matrix. J Biol Chem 2009; 284: 34935–34943.
17. Clément A, Wiweger M, von der Hardt S, et al. Regulation of zebrafish skeletogenesis by ext2/dackel and papst1/pinscher. PLoS Genet 2008; 4: e1000136.
18. Reijnders CM, Waaijer CJ, Hamilton A, et al. No haploinsufficiency but loss of heterozygosity for EXT in multiple osteochondromas. Am J Pathol 2010; 177: 1946–1957.
19. Zuntini M, Pedrini E, Parra A, et al. Genetic models of osteochondroma onset and neoplastic progression: evidence for mechanisms alternative to EXT genes inactivation. Oncogene 2010; 29: 3827–3834.
20. Jones KB, Piombo V, Searby C, et al. A mouse model of osteochondromagenesis from clonal inactivation of Ext1 in chondrocytes. Proc Natl Acad Sci USA 2010; 107: 2054–2059.
21. Matsumoto K, Irie F, Mackem S, et al. A mouse model of chondrocyte-specific somatic mutation reveals a role for Ext1 loss of heterozygosity in multiple hereditary exostoses. Proc Natl Acad Sci USA 2010; 107: 10932–10937.

22. Hilton MJ, Gutierrez L, Martinez DA, et al. EXT1 regulates chondrocyte proliferation and differentiation during endochondral bone development. Bone 2005; 36: 379–386.
23. de Andrea CE, Wiweger M, Prins F, et al. Primary cilia organization reflects polarity in the growth plate and implies loss of polarity and mosaicism in osteochondroma. Lab Invest 2010; 90: 1091–1101.
24. Vernier RL, Klein DJ, Sisson SP, et al. Heparan sulfate-rich anionic sites in the human glomerular basement membrane. Decreased concentration in congenital nephrotic syndrome. N Engl J Med 1983; 309: 1001–1009.
25. Hogendoorn PCW, De Heer E, Weening JJ, et al. Glomerular capillary wall charge and antibody binding in passive Heymann nephritis. J Lab Clin Med 1988; 111: 150–157.
26. Sauren YM, Mieremet RH, Groot CG, et al. Polyethyleneimine as a contrast agent for ultrastructural localization and characterization of proteoglycans in the matrix of cartilage and bone. J Histochem Cytochem 1991; 39: 331–340.
27. Schurer JW, Kalicharan D, Hoedemaeker PJ, et al. The use of polyethyleneimine for demonstration of anionic sites in basement membranes and collagen fibrils. J Histochem Cytochem 1978; 26: 688–689.
28. Kimmel CB, Ballard WW, Kimmel SR, et al. Stages of embryonic development of the zebrafish. Dev Dyn 1995; 203: 253–310.
29. Wiweger MI, Avramut C, de Andrea CE, et al. Cartilage ultrastructure in proteoglycan-deficient zebrafish mutants brings to light new candidate genes for human skeletal disorders. J Pathol 2011; 223:531-42.
30. Ueda H, Toriumi H, Leng CG, et al. A histochemical study of anionic sites in the intermediate layer of rat femoral cartilage using polyethyleneimine at different pH levels. Histochem J 1997; 29: 617–624.
31. Prins FA, Diemen-Steenvoorde R, Bonnet J, et al. Reflection contrast microscopy of ultrathin sections in immunocytochemical localization studies: a versatile technique bridging electron microscopy with light microscopy. Histochem 1993; 99: 417–425.
32. Sissoeff I, Grisvard J, Guille E. Studies on metal ions–DNA interactions: specific behaviour of reiterative DNA sequences. Prog Biophys Mol Biol 1976; 31: 165–199.
33. Sauren YM, Mieremet RH, Lafeber FP, et al. Changes in proteoglycans of ageing and osteoarthritic human articular cartilage: an electron microscopic study with polyethyleneimine. Anat Rec 1994; 240: 208–216.
34. Heinegard D. Proteoglycans and more—from molecules to biology. Int J Exp Pathol 2009; 90: 575–586.
35. Willems SM, Wiweger M, Frans Graadt van Roggen J, et al. Running GAGs: myxoid matrix revisited. What's in it for the pathologist? Virchow Arch 2009; 456: 181–192.

36. Heinegard D, Saxne T. The role of the cartilage matrix in osteoarthritis. Nat Rev Rheumatol 2011; 7: 50–56.
37. Esko JD, Kimata K, Lindahl U. Proteoglycans and sulfated glycosaminoglycans. In Essentials of Glycobiology, 2nd edn, Varki A, Cummings RD, Esko JD, et al. (eds). Cold Spring Harbor Laboratory Press: Cold Spring Harbor, NY, 2009.
38. Bianco P, Kuznetsov SA, Riminucci M, et al. Reproduction of human fibrous dysplasia of bone in immunocompromised mice by transplanted mosaics of normal and Gsα-mutated skeletal progenitor cells. J Clin Invest 1998; 101: 1737–1744.

Supporting Information

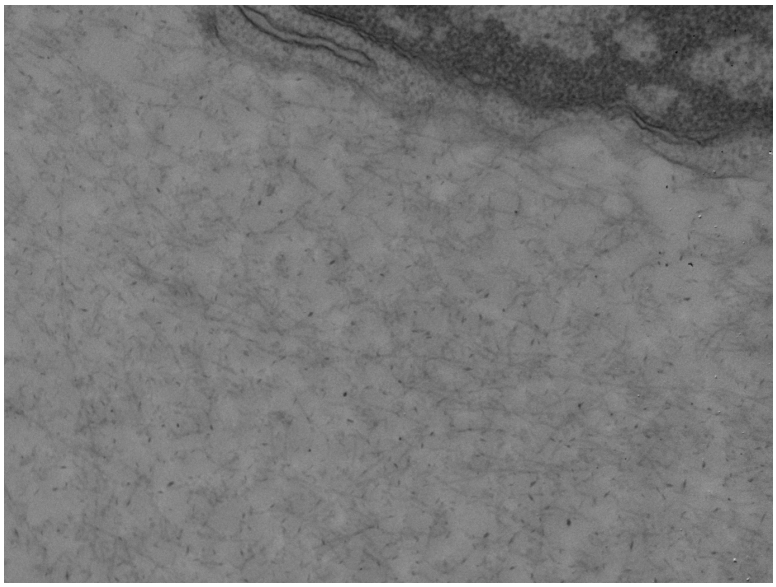

Supporting Information: Figure S1. Post-embedding PEI at pH 1.0, showing a virtual absence of stained anionic sites.